HHS Public Access

Author manuscript

Mol Cancer Ther. Author manuscript; available in PMC 2017 September 01.

Published in final edited form as:

Mol Cancer Ther. 2016 September ; 15(9): 2119–2129. doi:10.1158/1535-7163.MCT-16-0197.

Dual and specific inhibition of NAMPT and PAK4 by KPT-9274 decreases kidney cancer growth

Omran Abu Aboud[1], **Ching-Hsien Chen**[1], **William Senapedis**[3], **Erkan Baloglu**[3], **Christian Argueta**[3], and **Robert H. Weiss**[1,2,4]

[1]Division of Nephrology, Dept. of Internal Medicine, University of California, Davis, CA, USA, 95616

[2]Cancer Center, University of California, Davis, CA, USA, 95616

[3]Karyopharm Therapeutics, Inc, Newton, MA 02459

[4]Medical Service, Sacramento VA Medical Center, Sacramento, CA, USA, 95655

Abstract

Kidney cancer (or renal cell carcinoma, RCC) is the sixth most common malignancy in the US and one of the relatively few whose incidence is increasing. Due to the near universal resistance which occurs with the use of current treatment regimens, reprogrammed metabolic pathways are being investigated as potential targets for novel therapies of this disease. Borrowing from studies on other malignancies, we have identified the PAK4 and NAD biosynthetic pathways as being essential for RCC growth. We now show, using the dual PAK4/NAMPT inhibitor KPT-9274, that interference with these signaling pathways results in reduction of G2/M transit as well as induction of apoptosis and decrease in cell invasion and migration in several human RCC cell lines. Mechanistic studies demonstrate that inhibition of the PAK4 pathway by KPT-9274 attenuates nuclear β-catenin as well as the Wnt/β-catenin targets cyclin D1 and c-Myc. Furthermore, NAPRT1 downregulation which we show occurs in all RCC cell lines tested makes this tumor highly dependent on NAMPT for its NAD requirements, such that inhibition of NAMPT by KPT-9274 leads to decreased survival of these rapidly proliferating cells. When KPT-9274 was administered in vivo to a 786-O (VHL-mut) human RCC xenograft model, there was dose-dependent inhibition of tumor growth with no apparent toxicity; KPT-9274 demonstrated the expected on-target effects in this mouse model. KPT-9274 is being evaluated in a phase 1 human clinical trial in solid tumors and lymphomas which will allow this data to be rapidly translated into the clinic for the treatment of RCC.

CORRESPONDING AUTHOR: Dr. Robert H. Weiss, Division of Nephrology, Department of Internal Medicine, Genome and Biomedical Sciences Building, Room 6312, 451 Health Sciences Dr., University of California, Davis, CA. 95616, rhweiss@ucdavis.edu, Tel: 530-752-4010; FAX: 530-752-3791.

CONFLICT OF INTEREST

W.S., E.B., and C.A. are employees of Karyopharm and made suggestions on the manuscript but did not influence the direction of the research reported here. Some of the reagents in this study were ordered by Karyopharm and gifted to the Weiss laboratory.

INTRODUCTION

Kidney cancer, one of the few malignancies increasing in incidence in the US, has a poor response to currently available agents and therefore new therapies are urgently needed (1). Based on work from our group and others (2, 3), it is becoming evident that RCC is truly a metabolic disease such that exploitation of newly discovered altered metabolic pathways is a fertile area for therapeutic target discovery. In our continuing evaluation of such reprogramming, it has become apparent that two such pathways, PAK4/β-catenin and NAD synthesis, are important in RCC progression but as yet have not been evaluated with respect to potential therapeutic targeting in this disease.

Given that PAK signaling (4, 5) and NAD generation (6, 7) play key roles in survival, proliferation, and oncogenic transformation, the discovery of a dual inhibitor of these pathways begged its evaluation in RCC. PAK4 is a group II PAK isoform and shows ubiquitous tissue expression (4). PAK4, which is embryonic lethal in knockout mouse models, is fully activated when bound to Cdc42 leading to modulation of nucleo-cytosolic trafficking of β-catenin. Through a two-step process, PAK4 stabilizes and activates β-catenin transcription of Wnt target genes such as cyclin D which is essential in regulating cell proliferation (8), and c-Myc which regulates apoptosis (9, 10) and glutamine reprogramming (11, 12). While PAK4 signaling has been studied in some detail in other malignancies (13), its only evaluation in kidney cancer prior to the work described here was to show that it portended both recurrence and adverse prognosis in patients with post-nephrectomy non-metastatic clear cell renal cell carcinoma (ccRCC) (14).

Targeting the regeneration of NAD, which is an essential metabolite for sustaining energy production especially in rapidly proliferating cancer cells, has the potential to be a successful therapeutic strategy in cancer (6). In this scheme, inhibition of NAMPT, the rate limiting enzyme of one of the NAD biosynthesis salvage pathways utilizing nicotinamide, results in significant depletion of NAD which is a key cofactor in the TCA cycle, epigenetics (sirtuins), and DNA repair (PARP). Since NAPRT1 which controls the alternative NAD biosynthesis salvage pathway through nicotinic acid (NA or niacin) is often down-regulated in specific malignancies through epigenetic promoter silencing (6), these cancers become highly dependent on NAMPT activity, making NAMPT an attractive potential therapeutic target. Prior to our work described here, the NAD salvage pathway had not been studied in human RCC, although in a murine kidney cancer (RENCA) model, attenuation of NAD biogenesis showed anti-angiogenic properties (15).

In the current study we demonstrate that RCC cells and xenograft tissues utilize both PAK4 and NAD-biosynthesis pathways for survival and that a novel dual PAK4/NAMPT inhibitor, KPT-9274, decreases xenograft growth by specifically affecting these pathways. There were minimal KPT-9274 effects on the normal human RPTECs and no apparent toxicity *in vivo*. This compound is currently under evaluation in phase 1 human clinical trials for the safety, tolerability and efficacy for the treatment of solid tumor malignancies and NHL (NCT02702492), such that with the pre-clinical data in RCC shown here, it can be rapidly translated into the clinic for evaluation of RCC treatment.

MATERIALS AND METHODS

Materials

MTT solution, mouse monoclonal anti-β-actin, NA, NMN and NAD were obtained from Sigma (St. Louis, MO, USA). The antibodies against (PAK4, p-PAK4, β-catenin, p-β-catenin, cycline D1, c-Myc, β-actin (rabbit), PARP, Sirtuin 1) were from cell signaling Technology, Inc. (Beverly, MA, USA). Goat anti-mouse and goat anti-rabbit HRP conjugated IgG were obtained from Bio-Rad (Hercules, CA). Anti-NAMPT was from Bethyl Laboratories (Montgomery, TX, USA), anti-NAPRT1 was from Proteintech (Rosemont, IL 60018, USA). ECL Plus solution was from Thermo-Fisher Scientific (Waltham MA, USA). KPT-9274 and its vehicle were from Karyopharm Therapeutics (Newton, MA, USA). FK866 was from TOCRIS Biosciences. Sunitinib was obtained from LC laboratories (Woburn, MA).

Cell lines

All RCC cell lines (786-0, ACHN, Caki-1) and U-2 OS cells were purchased from American Type Culture Collection (Rockville, MD, USA) in 2013 and authenticated originally by the source using short tandem repeat (STR). Cells were expanded and then frozen at low passage within 4 weeks after the receipt of the original stocks. Thawed cells were used within 15 passages without further authentication for this study. The “normal human proximal epithelial kidney cell line” (RPTEC) was purchased from Lonza (Basel, Switzerland) in 2015, authenticated by STR by the source, and used within 8 passages. All cells were routinely monitored in our laboratory for cellular morphology and microbial presence by microscopic observation and they were mycoplasma tested after each thaw or every 6 weeks if they are growing in culture. RPTEC cells, 786-O and Caki-1 cells were all maintained in DMEM media supplemented with 10% FBS, 100 units/mL streptomycin, and 100 mg/mL penicillin. The cells were maintained at 5% CO_2 and at 37°C.

Enzymatic NAMPT Assay

For the effect of KPT-9274 on NAMPT activity, recombinant NAMPT activity was measured using a coupled-enzyme reaction system (CycLex NAMPT Colorimetric Assay Kit Cat# CY-1251: CycLex Co., Ltd., Nagano, Japan). The two-step protocol was used following the manufacturer’s instructions. Briefly, NAMPT was incubated with KPT-9274, in the presence of adenosine triphosphate (ATP), nicotinamide, phosphoribosyl pyrophosphate (PRPP), and nicotinamide nucleotide adenylyltransferase 1 (NMNAT1), for 60 minutes at 30 °C. Water-soluble tetrazolium salts (WST-1), alcohol dehydrogenase (ADH), diaphorase, and ethanol were then added to each sample for 30 minutes. Following the final incubation, the absorbance of the samples was detected at 450 nm using a Spectramax i3 (Molecular Devices) spectrometer and Softmaxpro software.

CRISPR silencing of PAK4

U-2 OS cells were cultured in McCoy’s 5A (Gibco) media supplemented with 10% FBS at 37°C with 5% CO_2. Cells were transfected (Lipofectamine 2000; Invitrogen) with a pair PAK4 of plasmids; one with a puromycin resistance gene and the other with GFP (Santa

Cruz Biotechnology cat# sc-401895) both including a gene encoding a D10A mutated Cas9 nuclease and a target-specific guide RNA (against PAK4). Briefly, 250,000 cells were plated in a single well of a 6-well plate and allowed to adhere overnight. The following day the cells were transfected in antibiotic free media and allowed to grow for 2 days. Selection was accomplished by culturing cells in 1 μg/mL of puromycin and visual selection of GFP. Individual puromycin resistant/GFP clones were isolated and PAK4 expression was determined using Western blot analysis.

Cell viability assay

Cell viability assay was performed as described previously (16). Briefly, 3,000 cells/well were plated in 96-well plates, and after the indicated treatments, the cells were incubated in MTT solution/media mixture. Then, the MTT solution was removed and the blue crystalline precipitate in each well was dissolved in DMSO. Visible absorbance of each well at 540 nm was quantified using a microplate reader.

Cell cycle analysis

Cell cycle analysis was performed utilizing Muse™ Cell Analyzer from Millipore (Billerica, MA) following manufacturer's instruction. Briefly, cells were cultured in T25 cell culture flasks and after 72h of the indicated treatments, the cells were washed with PBS, fixed in 70% ethyl alcohol for 3h and stained with propidium iodide (PI). After staining, the cells were processed for cell cycle analysis.

Apoptosis assay

Annexin V & Dead Cell Assay was performed utilizing Muse™ Cell Analyzer from Millipore (Billerica, MA) following manufacturer's instruction. Briefly, after the indicated 72h treatments, the cells were incubated with Annexin V and Dead Cell Reagent (7-AAD) and the events for dead, late apoptotic, early apoptotic, and live cells were counted.

Immunoblotting

Cell lysates and tissue lysates were prepared with RIPA or T-PER buffers, respectively from Fisher scientific (Grand Island, NY, USA) in the presence of protease inhibitor cocktail from Invitrogen. Immunoblotting was done as described previously (16). Briefly, after the indicated treatments, the cells were washed with PBS, lysed in their lysis buffer, and whole-cell lysates as well as cytoplasmic and nuclear extracts were immunoblotted. For the tissue immunoblotting, tissue was weighed, homogenized and sonicated in T-PER buffer. The nitrocellulose membranes were blocked in 5% nonfat dry milk for one hour at room temperature, incubated with indicated antibodies, and then probed with horseradish peroxidase tagged anti-mouse or anti-rabbit IgG antibodies. The signal was detected using ECL Plus solutions.

siRNA Transfection

Cells were plated in 6-well plates for immunoblotting or T25 flasks for apoptosis assays. After 24 hours, cell monolayers at approximately 60% confluency were subjected to siRNA transfection. The human PAK4 siRNA used is a smart-pool RNA, with 5 reference

sequences (ThermoFisher catalog S20135). The transfection mixture was prepared in Opti-MEM GlutaMax medium from Invitrogen (Carlsbad, CA, USA) with siRNA and Lipofectamine RNAiMAX according to the manufacturer's protocol. The final concentration of siRNA oligonucleotides (scrambled or PAK4) added to the cells were 25 nM. The cells were cultured in the presence of transfection mixture for 24h. The transfection mixture was replaced by fresh DMEM medium the following day, and cell culture was pursued for an additional 48 hours. After the transfection, cells were collected for immunoblotting, or apoptosis assays.

Transwell migration and invasion assays

The *in vitro* cell migration and invasion assays were performed using transwell chambers (8-mm pore size; Costar, Cambridge, MA). For the transwell migration assay, 1.5×10^4 cells were seeded on top of the polycarbonate filters, and 0.6 ml of growth medium with DMSO or KPT-9274 (1μM and 5μM) was added to both the upper and lower wells. After incubation for 12 hours, the filters were swabbed with a cotton swab, fixed with methanol, and then stained with Giemsa solution (Sigma-Aldrich, St Louis, MO). For the *in vitro* invasion assay, filters were coated with Matrigel (Becton Dickinson, Franklin Lakes, NJ), and 2.5×10^4 cells were seeded onto the Matrigel and incubated for 20 hours. The cells attached to the lower surface of the filter were counted under a light microscope (10× magnification).

Scratch wound-healing assay

786-O cells were seeded onto 12-well tissue culture dishes and grown to confluence. Each confluent monolayer was then wounded linearly using a pipette tip, and washed three times with PBS. Thereafter, cell morphology and migration were observed and photographed at regular intervals for 12 and 24 hours. The number of cells migrating into the cell-free zone was determined by light microscopy.

Immunofluorescent staining

Cells cultured on 12-mm glass cover-slips were fixed for 15 minutes in PBS containing 4% paraformaldehyde and 2% sucrose and then permeabilized in PBS containing 0.3% Triton X-100 for 2 minutes. Cover slips were reacted with primary antibody against β-catenin and FITC-labelled anti-rabbit secondary antibody. F-actin was stained with TRITC-conjugated phalloidin, and nuclei were demarcated with DAPI staining. The cells were mounted onto slides and visualized using fluorescence microscopy (model Axiovert 100; Carl Zeiss, Oberkochen, Germany) or a Zeiss LSM510 laser-scanning confocal microscope image system.

NAD+ and NADH measurement

Cells were plated at 3,000 cells/well in 96-well plates and incubated overnight. Media was removed, and replaced by fresh media containing compound at indicated treatments in triplicate. 48 hours later cells were lysed and total NAD and NADH was assayed by luminescence measurement using The NAD/NADH-Glo™ Assay (Promega, Madison) following the manufacturer's protocol.

In vivo experiments

All animal procedures were performed in compliance with the University of California Institutional Animal Care and Use Committee. Male athymic Nu/Nu mice (8 weeks of age and weight ~25 g) were injected with 786-O (human RCC) cells subcutaneously (DMEM:Matrigel 3:1) in the flank region. Tumor progression was monitored weekly by calipers using the formula: tumor volume in mm^3 = (length × $width^2$)/2. When tumor size reached approximately 225 mm^3, animals were randomly assigned to treatment groups and treatments were started (day one). KPT-9274 drug product (30% KPT-9274 API + 40% Polyvinylpyrrolidone K30 + 15% methyl cellulose + 15% Phospholipon 90G) or vehicle (58% Polyvinylpyrrolidone K30 + 21% methyl cellulose + 21% Phospholipon 90G) was administered by oral gavage twice daily for 5 days at 100 and 200 mg/kg twice a day. As a positive control, oral gavage of sunitinib in vegetable oil was given. Sunitinib was administered via oral gavage 5 days a week at 40mg/kg body weight. To determine any potential toxicity of the treatment(s), body weights of the animals were measured and signs of adverse reactions were monitored. On day 28 of treatment, the mice were euthanized and the tumor volume was determined: mm^3 = (length × $width^2$)/2

Bioanalysis of KPT-9274 in Mouse Plasma and 786-0 xenograft tumors

At the end of the experiment animals were dosed by vehicle or KPT-9274 and 8 hours later plasma and tumor tissues were collected. Vehicle or KPT-9274 Samples (n=6) were kept in −80 °C and sent to Cyprotex facility (Watertown, MA) for KPT-9274 analysis. Briefly, analysis was performed by LC/MS/MS using an Agilent 6410 mass spectrometer coupled with an Agilent 1200 HPLC and a CTC PAL chilled autosampler and peaks were analyzed by mass spectrometry (MS) using ESI ionization in MRM mode.

Statistical analysis

Comparisons of mean values were performed using the independent samples t-test. A p-value of < 0.05 was considered significant. For the *in vivo* studies a two-way ANOVA multiple comparison test was performed to compare the treatment groups and < 0.05 was considered significant.

RESULTS

KPT-9274 attenuates the PAK4/β-catenin pathway, results in NAD depletion, and attenuates viability, invasion, and migration in several RCC cell lines

KPT-9274 is an orally bioavailable small molecule (Fig. 1A) that shows dual inhibition of NAMPT and PAK4. To examine NAMPT and PAK4 target engagement, we first examined the ability of KPT-9274 to inhibit NAMPT and PAK4 activity. Inhibition of NAMPT in a cell-free enzymatic assay using recombinant NAMPT shows an IC_{50} of ~120 nM for KPT-9274 (Fig. 1B). CRISPR PAK4 knock-out in an U-2 OS cell line confirms inhibition of PAK4 as evidenced by a 6-fold resistance to KPT-9274-induced growth inhibition (measured by MTT assay) as compared to the parental cell line (Fig. 1C). We confirmed cellular inhibition of NAMPT as evidenced by reduction of total NAD after treatment two RCC cell lines with KPT-9274 (Fig. 1D), and we showed inhibition of PAK4 through dose-dependent

steady reduction in phospho-PAK4 by immunoblotting preferentially in RCC cell lines as compared to a primary normal renal tubular epithelial cell line (Fig. 1E).

Since gastrointestinal and other cancers (although not previously reported in RCC) have shown dependence on PAK4 via constitutive activation of the Wnt pathway (17) and because rapidly proliferating cancer cells require continuous replenishing of NAD for energy and DNA repair pathways (6), we asked whether there was a differential effect of KPT-9274 on survival between “normal” RPTEC and RCC cell lines *in vitro*. Viability of the two RCC cell lines showed striking dose-dependence of KPT-9274, with a cell viability IC_{50} of 600 nM for Caki-1 cells and 570 nM for 786-0 when incubated with the drug for 72 hours (Fig. 2A). By contrast, viability of the primary RPTEC cells derived from normal kidney was attenuated by 45% at 2–10 μM with an IC_{50} of 1300 nM) (Fig. 2A). This differential effect of KPT-9274 on RPTEC versus RCC cell lines suggest that the inhibited pathways are more active in malignant-derived than in normal cell lines and bodes well for tolerability in humans.

To evaluate additional cancer-related pathways, we evaluated cell invasion through Matrigel and cell migration using two methods. Given the lack of toxicity of KPT-9274 in 786-O cells for 24 hours with concentrations up to 5 μM (Supplementary Fig. 1), we assessed the effect of 1 μM and 5 μM KPT-9274 on cell invasiveness and motility in these cells. An *in vitro* invasion assay demonstrated a 2.2-fold and 3.9-fold decrease in cell invasiveness in response to KPT-9274 treatment at 1 μM and 5 μM, respectively (Fig. 2B), and 786-O cell migration was also decreased in KPT-9274 treated cells as compared to cells treated with the DMSO vehicle (Fig. 2C). A similar suppression of cell motility was observed in these cells incubated with KPT-9274 using a standard wound healing assay (Fig. 2D).

KPT-9274 attenuates G2/M transit and induces apoptosis in RCC cell lines

Since many Wnt/β-catenin target genes lie downstream of PAK4, such that PAK4 is indirectly involved in of a variety of proliferative and survival pathways (8), we next asked whether cell cycle progression and apoptosis in RCC cells were affected by KPT-9724. Using flow cytometry, we first evaluated cell cycle progression and showed that KPT-9274 causes a significant increase in the G2/M phase of the cell cycle in the RCC cells but not the RPTEC cells, as compared to the vehicle controls, suggesting arrest at this cell cycle stage in RCC (Fig. 3A; gating data shown in Supplementary Fig. 2).

While there was minimal but significant apoptosis as measured by annexin V flow cytometry in RPTEC cells treated with KPT-9274 when compared to vehicle control, the effect was more pronounced in both RCC cell lines treated with KPT-9274 (Fig. 3B). To further evaluate apoptosis, we observed significant PARP cleavage by immunoblot in the cancer cells with a more dramatic effect on the VHL-null 786-0 cells at both 72 and 96 hours, but no cleavage was observed in the RPTEC (Fig. 3C). Decreased PARP cleavage at the higher concentrations of KPT-9274 is likely due to the NAD dependence of PARP (18) in the presence of NAD biosynthesis inhibition by KPT-9274 (see below). Taken together these data indicate that KPT-9274 attenuates proliferation and enhances apoptotic pathways in RCC cells.

KPT-9274 affects RCC oncogenic signaling pathways and shows specify to PAK4 inhibition

To confirm specificity of the responses on the PAK4 pathway to KPT-9274 (see Fig. 1E), we utilized siRNA methods. SiRNA attenuation with a construct specific to PAK4 resulted in a decrease in PAK4, phospho-PAK4, and phospho-β-catenin in all cell lines (Fig. 4A). Interestingly, while the siRNA caused the expected changes in these proteins in normal RPTECs, KPT-9274 did not result in parallel changes in PAK4 and phospho-β-catenin in these cells (Fig. 1E), suggesting that the drug has differential sensitivity to members of these pathways on cancer as compared to normal cells. After PAK4 siRNA transfection, the annexin V flow cytometry showed similar results to KPT-9274 (Fig. 4B, compare to Fig. 3B). Taken together, these data are consistent with the likely lack of KPT-9274 effect in normal kidney parenchyma and suggest that there will be minimal toxicity of this inhibitor to normal tissues.

Both c-Myc and cyclin D1 are transcriptional targets of the Wnt ligand through nucleo-cytosolic shuttling of β-catenin through PAK4 (8), and in addition both of these genes are known to be activated in RCC oncogenesis and reprogramming (11, 12, 19). In further evaluation of oncologic-relevant players in the PAK4 pathway impacted by KPT-9274, we show that c-Myc and cyclin D1 are attenuated by KPT-9274 in RCC cell lines but not in the RPTEC cells (Fig. 4C).

On the basis of the observations showing reduced expression of β-catenin target genes (cyclin D1 and c-Myc) in KPT-9274-treated cells, we next asked whether KPT-9274 treatment regulates nuclear localization of β-catenin since this is the location where transcriptional activation properties of this protein are apparent (20). Immunofluorescence staining demonstrated an accumulation of β-catenin protein in the nucleus of DMSO-treated 786-O cells, whereas nuclear, and to some extent cytosolic, distribution of β-catenin was decreased in response to KPT-9274 (Fig. 4D). Confirmatory data from cytosolic/nuclear separated proteins, which shows higher resolution than immunoblotting of total β-catenin (Fig. 4A) showed a decrease of β-catenin protein in both the cytosolic and nuclear fractions of cells exposed to KPT-9274 with a higher decrement in nuclear β-catenin at the earlier time point (Fig. 4E).

NAD depletion in RCC cells is induced upon KPT-9274 treatment

The availability of abundant NAD is a key requirement in rapidly proliferating cancer cells and is produced through several biosynthetic pathways including the de novo pathway from tryptophan (most active in the liver; Pathway 1 in Fig. 5A) and two salvage pathways (Pathways 2 and 3 in Fig. 5A). However, in many cancer cells, NAD salvage achieved through NAPRT1 catalysis of nicotinic acid is downregulated and causes cellular energy requirements to be highly dependent on NAMPT for NAD regeneration and cell survival (6). To determine which pathways are in play in RCC, we evaluated protein levels of NAMPT and NAPRT1 by immunoblotting of several RCC cell lines as well as the normal RPTEC cells. While NAMPT levels were similar in both RCC cells used in this study as compared to RPTEC (Fig. 5B), NAPRT1 was markedly decreased in these cells (although less so in ACHN, derived from a human RCC pleural effusion) suggesting a critical dependence of RCC, but not RPTEC, on the NAMPT salvage pathway for its requisite supply of NAD; this

also represents the first demonstration of such reprogramming of the NAD synthetic pathway in RCC.

Since NAD is required for rapid proliferation of cancer cells, we next evaluated the results of NAMPT inhibition, and consequent NAD attenuation, after treatment with KPT-9274. Although RCC and RPTEC cells showed a marked decrease in total NAD species upon KPT-9274 incubation for 48 hours (Fig. 5C), nicotinic acid (the NAPRT1 substrate) rescued NAD levels in the RPTEC cells but not in the RCC cells lines, likely due to decreased expression of NAPRT1 (see Fig. 5B and Pathway 3 in Fig. 5A) in RCC. Additionally, NMN (nicotinic mononucleotide), which lies downstream of NAMPT (see Pathway 2 in Fig 5A), rescues NAD biosynthesis in all cell types (Fig. 5C). As a control for NAMPT inhibition, we utilized FK866, a selective NAMPT inhibitor, which showed similar effects to KPT-9274 on total NAD (Fig. 5C).

To demonstrate the requirement of NAD for survival of RCC cells, we evaluated cell viability under NAD-altering conditions similar to the above experiments. As above, we found that RCC cell viability was decreased by KPT-9274 and was rescued by the addition of NMN; there was no rescue of cell viability when NA was added on RCC cells incubated with KPT-9274 (Fig. 5D; compare to Fig. 5C). To further investigate and confirm the role of the NAD pathway in RCC, we evaluated levels of Sirt1, a NAD-dependent enzyme with multiple roles in cellular metabolism, senescence and DNA repair in many malignancies. Consistent with the inhibitory effect of KPT-9274 on the NAD pathway through NAMPT, Sirt1 levels were decreased after incubation of both RCC cell lines with this inhibitor, but Sirt1 levels were not affected in RPTEC cells (Fig. 5E). Taken together, these data demonstrate that RCC utilize the NAMPT salvage pathway to generate sufficient NAD for their energy requirements, and that KPT-9274 decreases NAD and viability levels through specific inhibition of NAMPT. RPTEC cells, on the other hand, can generate NAD through the NAPRT1 pathway despite inhibition of NAMPT by KPT-9274 and are thus less sensitive to this drug. This is confirmed by the ability of these cells to rescue NAD levels and cell viability when treated with KPT-9274 and supplied with NA at the same time (Fig. 5C, D).

KPT-9274 decreases tumor growth in a human xenograft model of RCC

In order to translate these *in vitro* findings to an *in vivo* model as a further step towards human trials, we utilized a xenograft model of human 786-O cells engrafted into nude mice. 500,000 cells/mouse were injected subcutaneously in 8 mice per condition. Once the tumors became visible (average size 234 mm^3), KPT-9274 formulated for oral delivery (30% KPT-9274 API + 40% Polyvinylpyrrolidone K30 + 15% methyl cellulose + 15% Phospholipon 90G) or vehicle (58% Polyvinylpyrrolidone K30 + 21% methyl cellulose + 21% Phospholipon 90G) was administered by oral gavage at 100 and 200 mg/kg twice daily for 5 days. As a positive control for tumor affect, oral gavage of sunitinib in vegetable oil was given once daily for 5 days at 40 mg/kg.

After 14 days of treatment, KPT-9274 demonstrated a decrement of xenograft growth (Fig. 6A) comparable to that of sunitinib (data not shown). As evidence for lack of toxicity, there was no significant weight loss in animals receiving KPT-9274 as compared to those receiving vehicle through the end of the experiment (Fig 6B). To confirm target effects of

KPT-9274, all tumors were immunoblotted for PAK4. The animals treated with KPT-9274 showed marked attenuation of PAK4 (Fig. 6C). Consistent with previous results, levels of PAK4 (see Fig. 1E), cyclin D1, and sirt1 (see Fig. 4C and 5E) were also decreased. To determine disposition of the inhibitor, levels of KPT-9274 were measured at the end of the experiment in mouse plasma and tumors and were found to be present in both blood and tissue at a similar magnitude (10757 ng/ml and 10647 ng/ml in plasma and tumor, respectably, 8 h after the last dose of KPT-9274).

DISCUSSION

Due to the historically poor response of RCC to immune-modulating therapies and the frequent resistance of RCC to current targeted therapeutics, the discovery of novel targetable pathways and small molecule inhibitors in RCC would represent a major advance in the field. The dual PAK4/NAMPT modulator, KPT-9274, targets two signaling pathways which have been described to be active and of importance in malignancy in general, yet neither of these pathways had previously been studied in detail in RCC. We now show that both of these pathways are highly active in RCC, and hence this inhibitor is ideally suited for further study in RCC including in human clinical trials.

The PAK4 pathway, by means of its effect on β-catenin, influences the transcription of such key Wnt-regulated proliferative and survival pathways as c-Myc and cyclin D1. PAK4 is active in various malignancies but until now, other than demonstration of overexpression in several renal cell lines (21), this pathway has not been thoroughly evaluated in RCC. With regard to NAD, an essential metabolite for sustaining cellular energy critical to the survival of rapidly proliferating cells, KPT-9274 attenuates a key arm of NAD biosynthesis. In malignancies such as RCC in which we now show that one of the pathways of synthesis (NAPRT1) is reprogrammed “down”, the end result of KPT-9274 inhibition contributes to poor survival of RCC cells and tissues likely due in part to limiting NAD biosynthesis (see Fig. 5A).

The family of p21-activated protein kinases (PAKs) is composed of serine-threonine kinases whose activity is regulated by the small p21 guanosine triphosphatases (GTPases) Rac1 and Cdc42. In turn PAK4, can also down-regulate the p21 cell cycle regulator, CDKN1A (22). The PAK proteins have been classified as group I and group II, and are positioned at the intersection of several important oncogenic pathways, including hallmarks of cancer such as growth signal autonomy, evasion of apoptosis, and promotion of invasion and metastasis (4). PAK4, the first of the group II PAKs to be cloned and characterized, is embryonic lethal in mice when knocked out and is critical to cytoskeletal organization (5). Subsequent investigation of this kinase showed that, by virtue of its regulation of nuclear import of β-catenin, it was capable of modulating transcription of β-catenin target genes such as cyclin D1 and c-Myc (8) which play key roles in cancer proliferation and metabolic reprogramming (11, 12, 19). Furthermore, through phosphorylation of CDK1NA, PAK4 can regulate cell cycle transit at G1/S and G2/M (23, 24). From a clinical standpoint and consistent with our data, those patients with relatively high PAK4 expression by immunohistochemistry of non-metastatic RCC in fact showed poorer prognosis (14).

NAD is briskly turned over in cancer cells which utilize this cofactor for energy requirements in rapidly proliferating cells, as well as by such NAD utilizing enzymes essential for cancer cell function (i.e. PARPs and SIRTs) (25); the most efficient biosynthesis of this cofactor occurs through the salvage pathways (6). Our data demonstrating the use by RCC cells of the salvage pathways rather than de novo synthesis from tryptophan for NAD biosynthesis are consistent with that seen in other cancers (6). We have shown that NAPRT1 is downregulated in all RCC cells tested (see Fig. 5C), leading to a reliance of these cells on NAMPT as is evidenced by the profound effects of KPT-9274 on these cells. As far as we can tell, this attenuation of NAPRT1 levels is the first report of a reprogrammed NAD biosynthesis pathway in RCC. These data also support the hypothesis that the salvage pathways, rather than the de novo pathway which occurs predominantly in the liver (26), are more highly represented in RCC. The fact that NA can be utilized by normal epithelial cells and sustain normal NAD levels when KPT-9274 is administrated makes this drug a good clinical candidate for RCC. Using KPT-9274 with NA supplementation when treating RCC will reduce the side effects of blocking NAMPT and subsequent NAD depletion in normal tissue.

Toxicology studies conducted in dogs and rats revealed the expected toxicities to the gastrointestinal tract and hematological cells (e.g. thrombocytopenia) which are common to other inhibitors of PAK4 or NAMPT (4–6). However, gross toxicity was not observed in the current efficacy study in mice although blood counts were not measured. The reason for the lack of observed toxicity may be that, while both PAK4 and NAD biosynthesis are essential in embryogenesis and for rapidly growing cell metabolism, these pathways are of relatively less importance in adult tissue homeostasis. It is also possible that dual inhibition at lower levels could ameliorate toxicities which occur at higher levels of single pathway inhibition. Safety and tolerability of KPT-9274 is currently being investigated in a Phase 1 human clinical trial of patients with advanced solid malignancies and NHL (clinicaltrials.gov; NCT02702492). Thus, translation of these inhibitors to human trials holds considerable promise for RCC.

Supplementary Material

Refer to Web version on PubMed Central for supplementary material.

Acknowledgments

FINANCIAL SUPPORT

This work was supported by NIH grants 1R01CA135401-01A1, 1R03CA181837-01, and 1R01DK082690-01A1, the Medical Service of the US Department of Veterans' Affairs, and Dialysis Clinics, Inc. (DCI) (all to R.H.Weiss). A non-restricted gift for research purposes was provided by Karyopharm Therapeutics, Inc.

We thank Drs. Vicki Huang and Xiaonan Chen for helpful suggestions and assistance with the experiments and the manuscript.

Reference List

1. Wettersten HI, Weiss RH. Potential biofluid markers and treatment targets for renal cell carcinoma. Nat Rev Urol. 2013; 10:336–44. [PubMed: 23545813]

2. Wettersten HI, Hakimi AA, Morin D, Bianchi C, Johnstone ME, Donohoe DR, et al. Grade-dependent metabolic reprogramming in kidney cancer revealed by combined proteomics and metabolomics analysis. Cancer Res. 2015; 75:2541–52. [PubMed: 25952651]

3. Hakimi AA, Reznik E, Lee CH, Creighton CJ, Brannon AR, Luna A, et al. An Integrated Metabolic Atlas of Clear Cell Renal Cell Carcinoma. Cancer Cell. 2016; 29:104–16. [PubMed: 26766592]

4. Radu M, Semenova G, Kosoff R, Chernoff J. PAK signalling during the development and progression of cancer. Nat Rev Cancer. 2014; 14:13–25. [PubMed: 24505617]

5. Dart AE, Wells CM. P21-activated kinase 4--not just one of the PAK. Eur J Cell Biol. 2013; 92:129–38. [PubMed: 23642861]

6. Sampath D, Zabka TS, Misner DL, O'Brien T, Dragovich PS. Inhibition of nicotinamide phosphoribosyltransferase (NAMPT) as a therapeutic strategy in cancer. Pharmacol Ther. 2015; 151:16–31. [PubMed: 25709099]

7. Ying W. NAD+/NADH and NADP+/NADPH in cellular functions and cell death: regulation and biological consequences. Antioxid Redox Signal. 2008; 10:179–206. [PubMed: 18020963]

8. Li Y, Shao Y, Tong Y, Shen T, Zhang J, Li Y, et al. Nucleo-cytoplasmic shuttling of PAK4 modulates beta-catenin intracellular translocation and signaling. Biochim Biophys Acta. 2012; 1823:465–75. [PubMed: 22173096]

9. Yuneva M, Zamboni N, Oefner P, Sachidanandam R, Lazebnik Y. Deficiency in glutamine but not glucose induces MYC-dependent apoptosis in human cells. J Cell Biol. 2007; 178:93–105. [PubMed: 17606868]

10. Shim H, Chun YS, Lewis BC, Dang CV. A unique glucose-dependent apoptotic pathway induced by c-Myc. Proc Natl Acad Sci U S A. 1998; 95:1511–6. [PubMed: 9465046]

11. Gao P, Tchernyshyov I, Chang TC, Lee YS, Kita K, Ochi T, et al. c-Myc suppression of miR-23a/b enhances mitochondrial glutaminase expression and glutamine metabolism. Nature. 2009; 458:762–5. [PubMed: 19219026]

12. Shroff EH, Eberlin LS, Dang VM, Gouw AM, Gabay M, Adam SJ, et al. MYC oncogene overexpression drives renal cell carcinoma in a mouse model through glutamine metabolism. Proc Natl Acad Sci U S A. 2015

13. Senapedis W, Crochiere M, Baloglu E, Landesman Y. Therapeutic Potential of Targeting PAK Signaling. Anticancer Agents Med Chem. 2015; 16:75–88. [PubMed: 26081410]

14. Liu W, Yang Y, Liu Y, Liu H, Zhang W, Xu L, et al. p21-Activated kinase 4 predicts early recurrence and poor survival in patients with nonmetastatic clear cell renal cell carcinoma. Urol Oncol. 2015; 33:205–21. [PubMed: 25744653]

15. Drevs J, Loser R, Rattel B, Esser N. Antiangiogenic potency of FK866/K22. 175, a new inhibitor of intracellular NAD biosynthesis, in murine renal cell carcinoma. Anticancer Res. 2003; 23:4853–8. [PubMed: 14981935]

16. Inoue H, Hwang SH, Wecksler AT, Hammock BD, Weiss RH. Sorafenib attenuates p21 in kidney cancer cells and augments cell death in combination with DNA-damaging chemotherapy. Cancer Biol Ther. 2011; 12

17. Cadoret A, Ovejero C, Terris B, Souil E, Levy L, Lamers WH, et al. New targets of beta-catenin signaling in the liver are involved in the glutamine metabolism. Oncogene. 2002; 21:8293–301. [PubMed: 12447692]

18. Houtkooper RH, Canto C, Wanders RJ, Auwerx J. The secret life of NAD+: an old metabolite controlling new metabolic signaling pathways. Endocr Rev. 2010; 31:194–223. [PubMed: 20007326]

19. Nigg EA. Cyclin-dependent protein kinases: key regulators of the eukaryotic cell cycle. Bioessays. 1995; 17:471–80. [PubMed: 7575488]

20. Jamieson C, Sharma M, Henderson BR. Targeting the beta-catenin nuclear transport pathway in cancer. Semin Cancer Biol. 2014; 27:20–9. [PubMed: 24820952]

21. Callow MG, Clairvoyant F, Zhu S, Schryver B, Whyte DB, Bischoff JR, et al. Requirement for PAK4 in the anchorage-independent growth of human cancer cell lines. J Biol Chem. 2002; 277:550–8. [PubMed: 11668177]

22. Nekrasova T, Minden A. PAK4 is required for regulation of the cell-cycle regulatory protein p21, and for control of cell-cycle progression. J Cell Biochem. 2011; 112:1795–806. [PubMed: 21381077]

23. Weiss RH. p21Waf1/Cip1 as a therapeutic target in breast and other cancers. Cancer Cell. 2003; 4:425–9. [PubMed: 14706334]

24. Niculescu AB III, Chen X, Smeets M, Hengst L, Prives C, Reed SI. Effects of p21(Cip1/Waf1) at both the G1/S and the G2/M cell cycle transitions: pRb is a critical determinant in blocking DNA replication and in preventing endoreduplication. Mol Cell Biol. 1998; 18:629–43. [PubMed: 9418909]

25. Schreiber V, Dantzer F, Ame JC, de MG. Poly(ADP-ribose): novel functions for an old molecule. Nat Rev Mol Cell Biol. 2006; 7:517–28. [PubMed: 16829982]

26. Heyes MP, Chen CY, Major EO, Saito K. Different kynurenine pathway enzymes limit quinolinic acid formation by various human cell types. Biochem J. 1997; 326(Pt 2):351–6. [PubMed: 9291104]

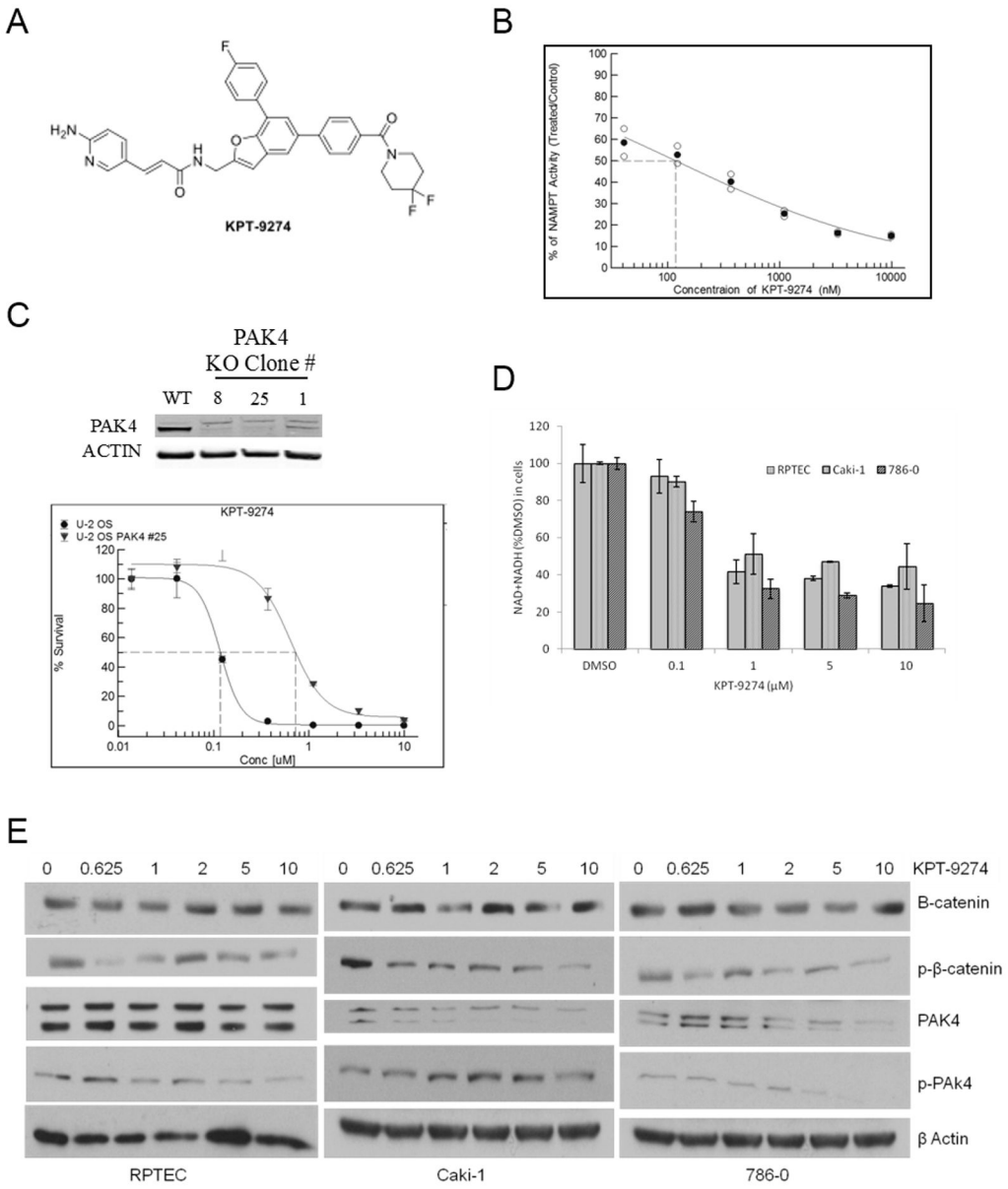

Figure 1.

KPT-9274 inhibits NAMPT and PAK4 and associated signaling pathways in RCC cells.

A. Molecular structure of KPT-9274

B. Cell-free assay of NAMPT activity as a function of KPT-9274 concentration

C. CRISPR-Cas9 splicing out of PAK4 in U-2 osteosarcoma cells showing the expected immunoblot and a shift to the right in the survival curve assessed by MTT assay.

D. NAD+NADH assay: 300 cells/well were plated in 96 well plates (n=4) and incubated for 48h with DMSO or KPT-9274. Assays of total NAD+NADH were performed in RCC cell lines as well as a normal primary renal proximal tubular epithelial cell (RPTEC) line as described in Materials and Methods. Error bars are SD.

*$p<0.05$ compared to DMSO treated controls. The black sold line indicates treatments significantly different compared to DMSO alone.

E. Immunoblotting of the cell lysates with the indicated antibodies was performed. Cells were plated in 6-well (1000 cells/well) and incubated with different concentrations of KPT-9274 for 72h before they lysed for protein extraction.
The experiments shown are representative of at least three independent repeats.

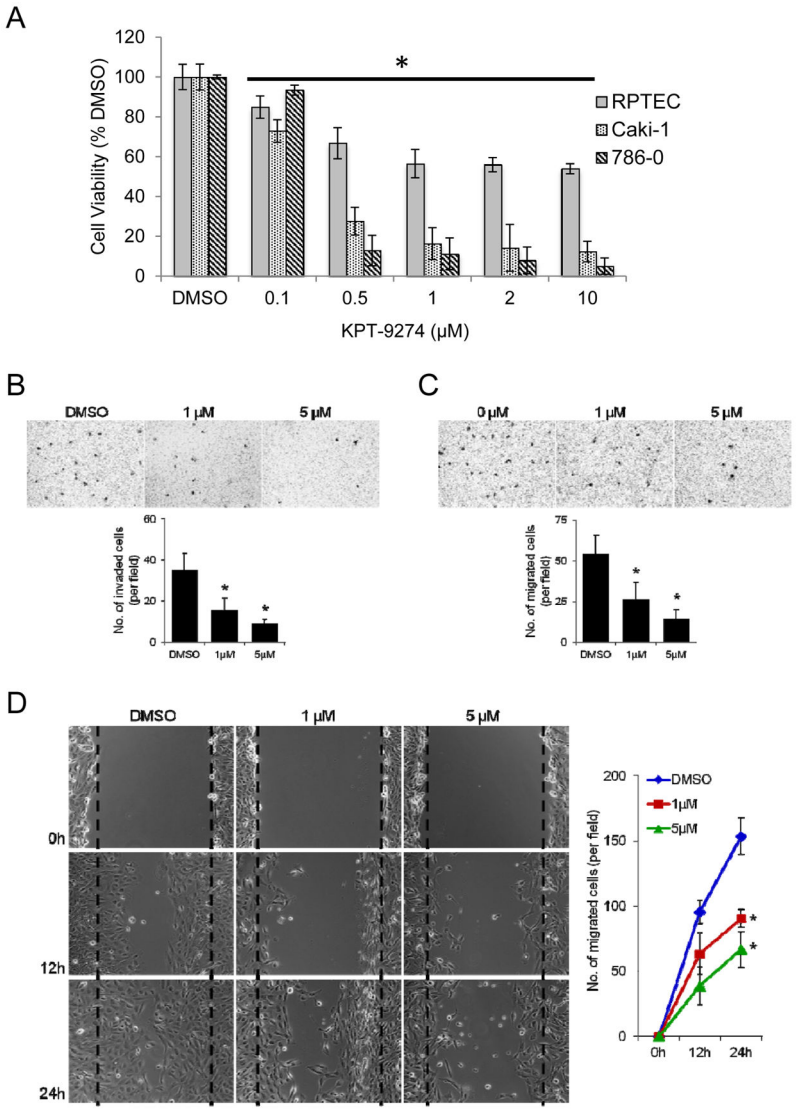

Figure 2.

KPT-9274 preferentially attenuates RCC cell viability and decreases RCC invasion and migration.

A. Both RCC cell lines in addition to a normal primary renal primary proximal tubular epithelial cell line (RPTEC) were plated in 96 well plates (3000 cells/well, n=8) and incubated 72h with DMSO or KPT-9274 before MTT was performed. Error bars are SD. *p<0.05 compared to DMSO treated controls. The black sold line indicates treatments significantly different compared to DMSO alone. The experiment shown is representative of at least three independent repeats.

B–D: 786-O cells were treated with DMSO, 1μM or 5μM KPT-9274 for 24 hours and then subjected to Matrigel invasion (**B**), transwell migration (**C**) and scratch/wound healing (**D**) assays.

(B) DMSO- or KPT-9274-treated cells were seeded on Matrigel-coated transwells with DMSO or KPT-9274; 20 hours later, migrated cells were fixed, stained, and counted using

light microscopy. A representative picture of each group is shown in the *top. Bottom*, quantification of migrated cells to the lower chamber. Data were presented as the mean value from six different fields ± SD (n = 3), $*p < 0.05$ as compared to DMSO-treated cells. **(C)** Migration assay in transwell chambers. Cells that migrated from the upper well of a transwell chamber into the lower well were stained, photographed (*top*) and counted (*bottom*). n = 3, $*p < 0.05$ versus DMSO group. **(D)** Confluent cultures of these cells were scratched and wound healing repair was monitored microscopically examined at 12 and 24 hours after the scratch and the addition of DMSO or KPT-9274. *Left*, representative phase contrast pictures. *Right*, numbers of cells migrated to the wound area were quantified at 0, 12 and 24 hours post-scratching (n = 3, $*p < 0.05$ versus DMSO-treated cells).

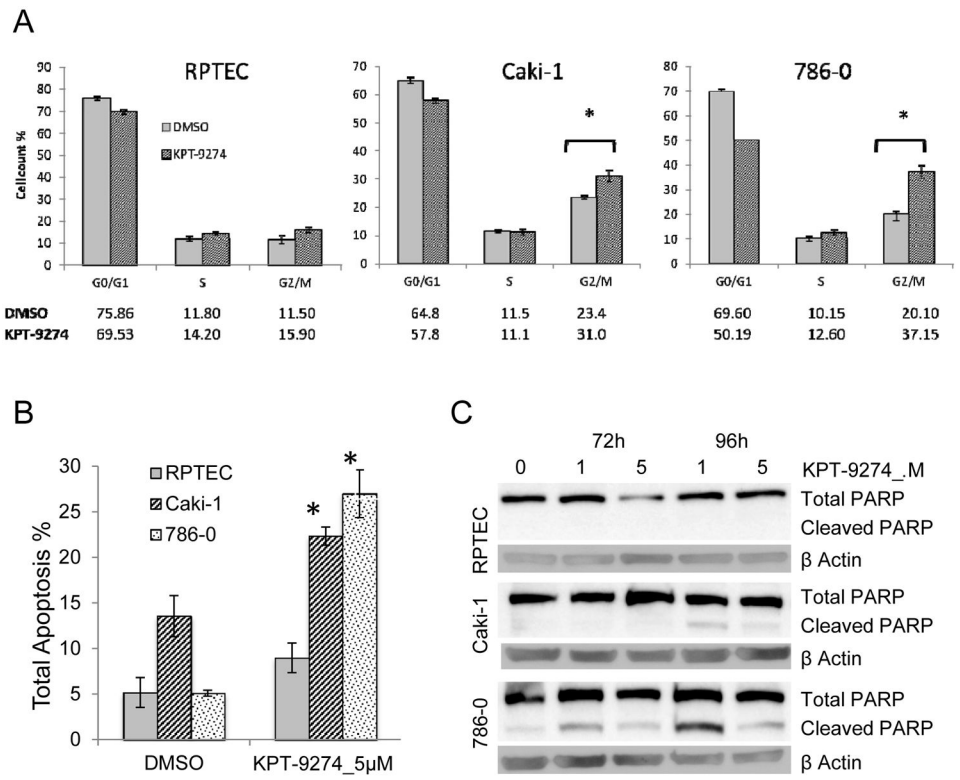

Figure 3.

KPT-9274 decreases G2/M transit and causes apoptosis preferentially in RCC cells.

Both RCC cell lines in addition to a normal primary renal proximal tubular epithelial cell line (RPTEC) were grown to 50% confluence and subjected to cell cycle analysis or apoptosis assays:

a. Cells were incubated with DMSO or KPT-9274 (5 μM) for 72h and analyzed with the Muse Analyzer for cell cycle analysis as described in Materials and Methods. The percentage of cells in each cell cycle phase was plotted. *$p<0.05$ KPT-9274 as compared to DMSO treatment

b. After incubation with KPT-9274 for 72h cells, annexin-V staining was used to measure total apoptosis by the Muse Analyzer as described in Materials and Methods. *$p<0.05$ as compared to DMSO treatment.

c. Immunoblotting of total and cleaved PARP in RPTEC and RCC cells KPT-9274 treated after 72h and 96h.

All results represent at least three independent experiments.

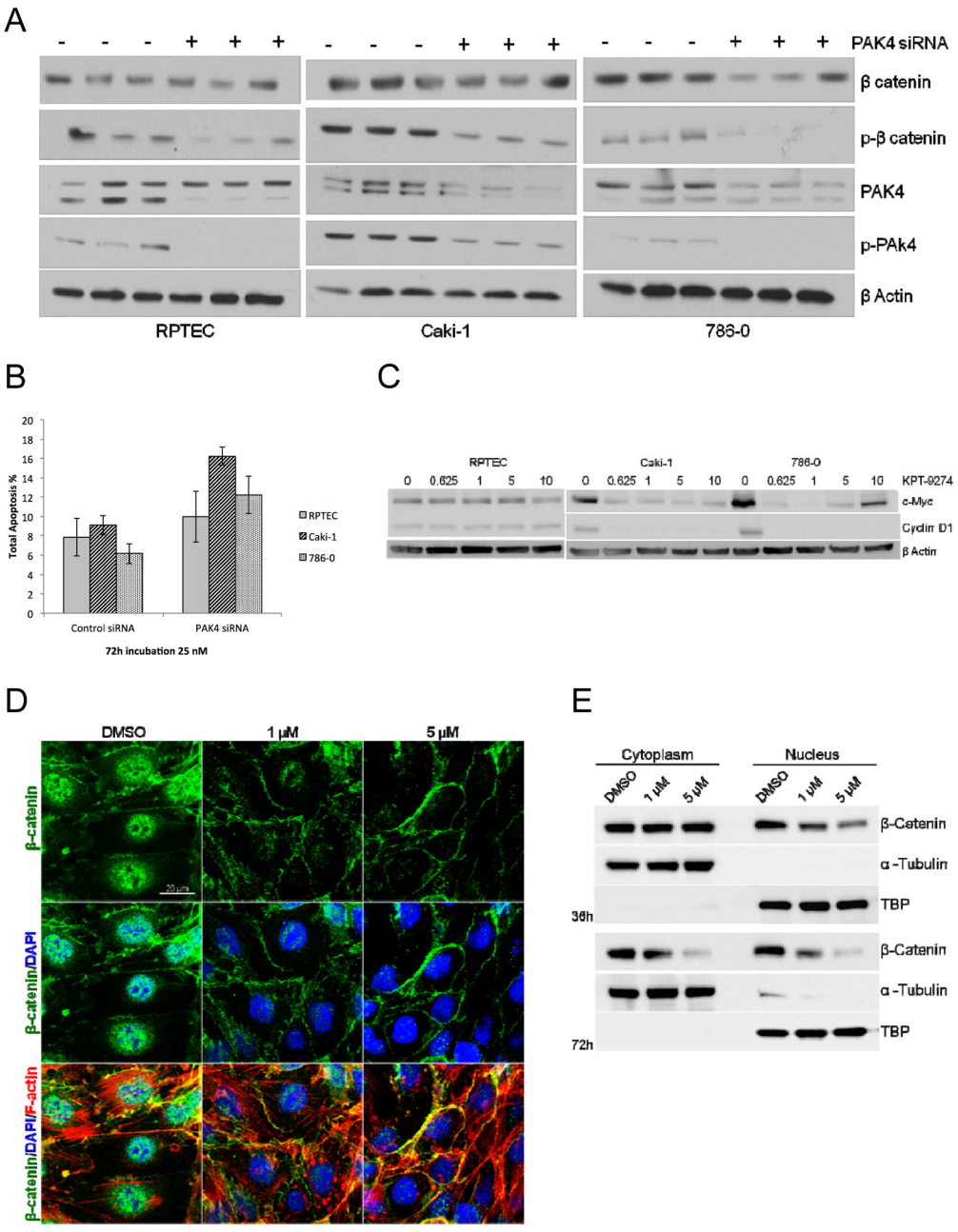

Figure 4.

KPT-9274 shows specificity for attenuation of PAK4 targets preferentially in RCC cells. Both RCC cell lines in addition to a normal primary renal proximal tubular epithelial cell line (RPTEC) were grown to 50% and transfected with an siRNA specific to PAK4 or a scrambled sequence control siRNA, then subjected to:

A. immunoblotting and

B. apoptosis assay by flow cytometry.

C. Whole cell lysates were immunoblotted with the indicated antibodies after incubation of the cells with the indicated concentrations of KPT-9274.

D. The subcellular localization of β-catenin in 786-O cells was determined by immunofluorescent staining after 24 hours of treatment with DMSO, 1μM or 5μM KPT-9274. The fluorescence of FITC-conjugated β-catenin (green), TRITC-conjugated phalloidin (F-actin stained: red) and DAPI (nucleus counter-stained: blue) was visualized under a confocal laser-scanning microscope. Scale bar: 20 μm

E. Western blot analysis of β-catenin in the cytosolic and nuclear portions of 786-O cells exposed to DMSO or KPT-9274 for 36 and 72 hours. TBP=TATA-Binding Protein, a nuclear constituent. Please see Materials and Methods for details.

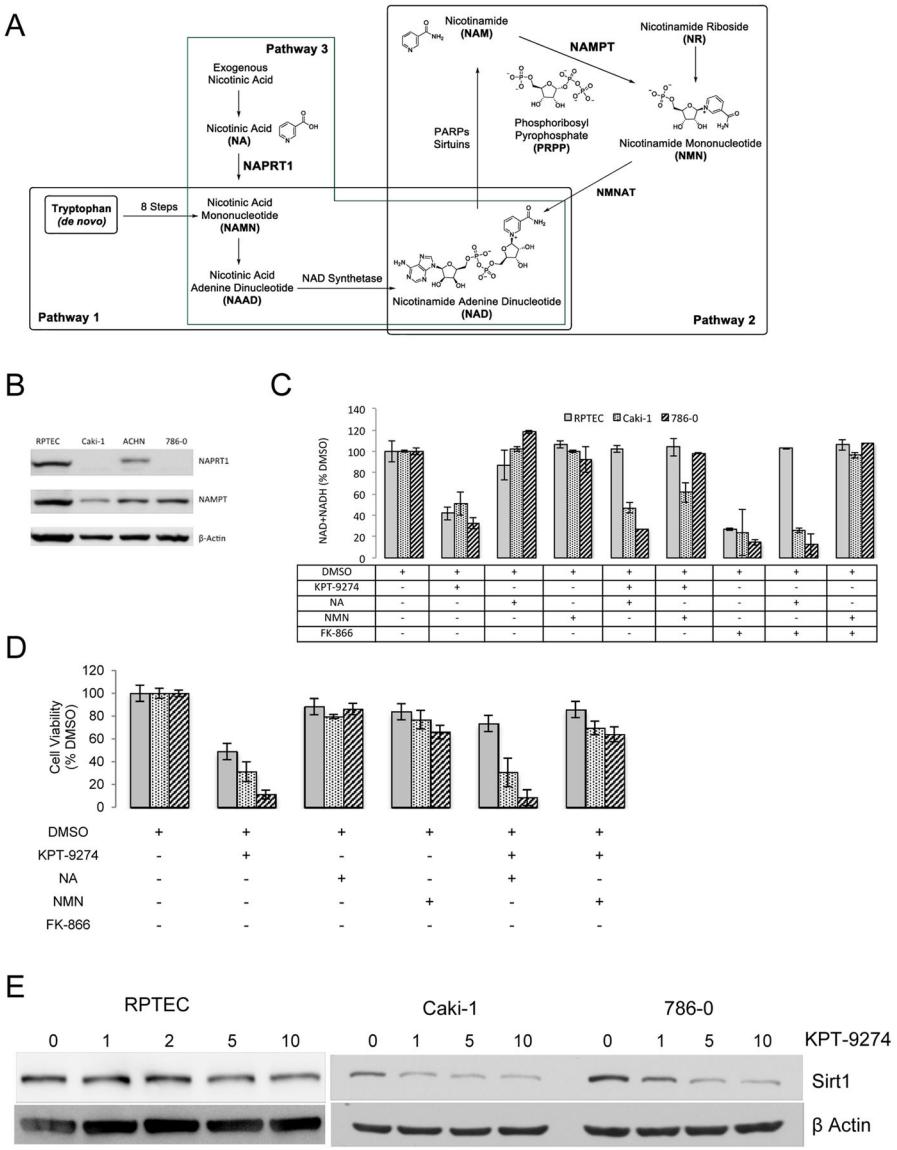

Figure 5.

KPT-9274 shows specificity for attenuation of NAD biosynthesis targets preferentially in RCC cells.

A. Schema of NAD biosynthesis from de novo (Pathway 1) and salvage pathways (Pathways 2 and 3).

B. Whole cell lysates from non-treated RCC and RPTEC cells were immunoblotted with the indicated antibodies.

C. Cells were grown in 96 well plates (300 cells/well), incubated as indicated, and subjected to assays for NAD+NADH as described in the Materials and Methods section.

D. Cells were grown in 96 well plates (300 cells/well, n=4), incubated as indicated, and subjected to MTT assays as described in the Materials and Methods section..

E. Cells were grown in 6 well plates (10,000 cells/well) exposed to KPT-9274 at the indicated concentrations (μM) for 72h and whole cell lysates were immunoblotted with sirt1 antibody.

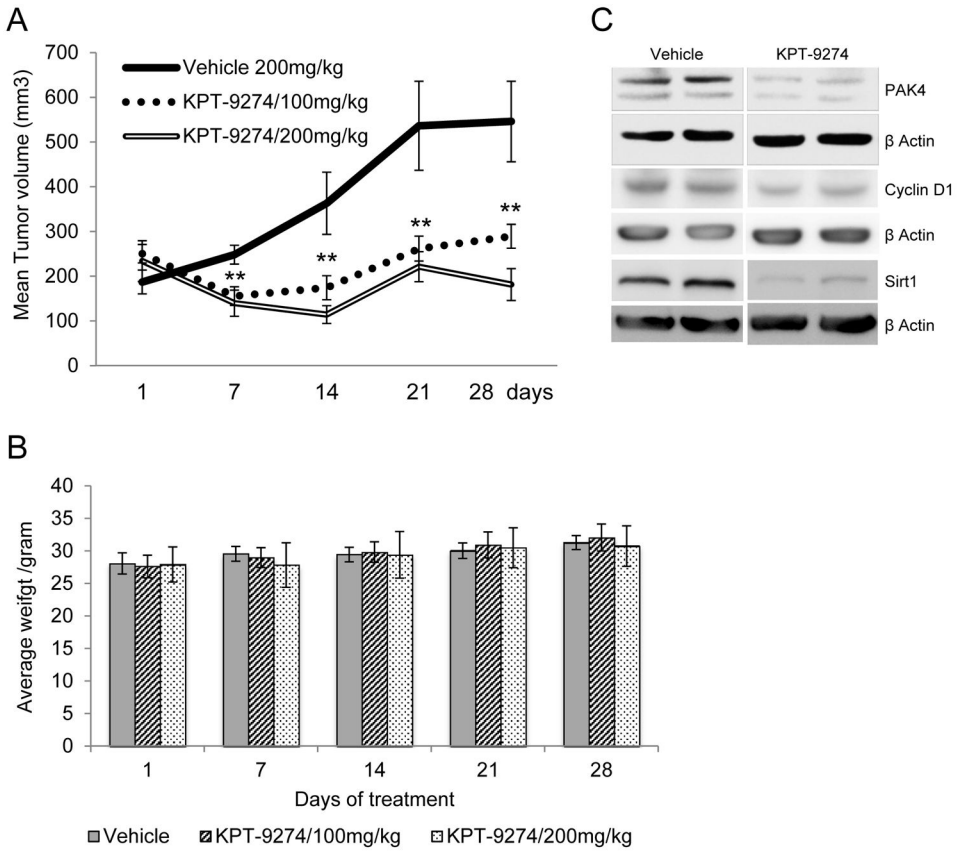

Figure 6.

KPT-9274 attenuates xenograft growth *in vivo* with minimal toxicity and shows the expected on-target effects.

A. Nude mice (n=8 per condition) were xenografted subcutaneously with 786-O cells and gavaged with KPT-9274 (100mg/kg or 200 mg/kg twice a day). Tumors were measured with calipers weekly at the times indicated and the mean tumor volumes ± SEM was calculated as described in Materials and Methods.

**$p<0.05$ indicates significant decrease in tumor volume compared to vehicle only group.

B. Mouse weights were determined at the time points indicated.

C. Tumors were harvested at sacrifice, pooled, and immunoblotted with the target antibodies indicated as well as β-actin as loading control.